

## Article

# New High Efficiency and Strength Bending Strain Sensor Based on Piezoelectric Stacks

Vladimir Sidorov , Nelly Rogacheva and Yulia Zheglova \*

Institute of Digital Technologies and Modeling in Construction, Moscow State University of Civil Engineering, Yaroslavskoye Shosse, 26, 129337 Moscow, Russia; sidorovvn@mgsu.ru (V.S.); rogachevann@mgsu.ru (N.R.)

\* Correspondence: jeglovayug@mgsu.ru; Tel.: +7-905-739-62-95

**Abstract:** This article is devoted to a mathematical model of a new piezoelectric sensor used for measuring bending strains. The first simple model of a piezoelectric sensor of bending deformations (we will call it a classical sensor) was presented in our previous paper. The classical sensor is a one-dimensional three-layer structure, in which the two outer layers are made of piezoelectric ceramic with preliminary polarization across the thickness of the sensor, and one elastic middle layer is located between these piezoelectric layers. In the present modified model of the new sensor, piezoelectric stacks are used instead of simple piezoelectric elements. As shown in the paper, this kind of piezoelectric composite sensor with stacks allows us to significantly increase the value and stability of the measured electrical signal and increase the accuracy of strains measurement. Piezoelectric ceramic is a brittle material. The use of stacks significantly reduces brittleness by enclosing thin layers of piezoelectric ceramic in a metal matrix. Piezoelectric laminated stacks have a periodic structure, and we will use the mathematical homogenization method to correctly determine their effective moduli (physical constants). Increasing the reliability of the proposed sensors, as well as the accuracy and stability of their deformation measurements, is aimed at enhancement of the mechanical safety of building structures, increasing the efficiency of their monitoring. The most important characteristic of any sensor is its efficiency. Our first classical bending strain sensor has a simple structure and an efficiency approaching the value of the coupling coefficient  $k_{31}$  ( $k_{31}$  is a constant describing a known physical property of a piezoelectric material). Our classic piezoelectric flexural strain sensor has an efficiency of the order of the coupling coefficient  $k_{31}$ . For piezoelectric materials with a strong piezoelectric effect, the  $k_{31}$  value is approximately 0.30–0.35. The efficiency of our classical sensor is hundreds of times greater than the efficiency of the most popular tangential (longitudinal) strain sensor, developed by Lord Kelvin. The efficiency of the flexural strain sensor using stacks is of the order of the coupling coefficient  $k_{33}$ . For the sensor with piezoelectric stacks, the value of efficiency is approximately 0.60–0.70. Note that the efficiency of the improved sensor is twice as high as the efficiency of our classic flexural strain sensor.



**Citation:** Sidorov, V.; Rogacheva, N.; Zheglova, Y. New High Efficiency and Strength Bending Strain Sensor Based on Piezoelectric Stacks. *Buildings* **2024**, *14*, 3814. <https://doi.org/10.3390/buildings14123814>

Academic Editor: Tinghua Yi

Received: 27 October 2024

Revised: 21 November 2024

Accepted: 26 November 2024

Published: 28 November 2024

**Keywords:** piezoelectric sensor of bending strains; piezoelectric stacks; homogenization method; effective moduli of stacks; sensor efficiency



**Copyright:** © 2024 by the authors. Licensee MDPI, Basel, Switzerland. This article is an open access article distributed under the terms and conditions of the Creative Commons Attribution (CC BY) license (<https://creativecommons.org/licenses/by/4.0/>).

## 1. Introduction

Experimental research plays an important role in the design and operation of structures. In this case, experimental and computational methods are used together, complementing each other.

Experimental research allows us to gather data on the distribution of stresses and deformations of a structure during operation to determine the stress-strain state of a structure of a very complex shape, which is difficult even with the use of modern computational methods and computers.

The first strain sensor was created by Professor Thomson in the middle of the 19th century. For his outstanding achievements in science, Professor Thomson received a new

name from the English Queen—Lord Kelvin. Lord Kelvin was the first to notice that the deformation of a conductor is accompanied by a change in its electrical resistance. By measuring the change in resistance, its deformation can be found. The first strain sensor—Lord Kelvin’s strain sensor—is based on this fact. The change in resistance is extremely small, but it can be amplified and measured using additional equipment.

Along with the widely used method of tensometry, other methods, such as photoelasticity, holographic and laser speckle interferometry, Moiré interferometry, optical heterodyne technology, and others, have been developed. The emergence of new materials and new directions in science, such as piezoelectric materials and electroelasticity, has led to new developments in experimental mechanics. One of these new branches of experimental mechanics is related to various piezoelectric sensors, which are based on the direct piezoelectric effect [1–6]. Currently, piezoelectric sensors are widely used in construction [7–11], and in many areas of modern technology [12,13].

Lord Kelvin’s strain sensor and piezoelectric strain sensors measure strains in the plane of the sensor. They allow us to determine the strains of extension, compression, and shear on the surface of the structure. As a result of their measurements, we determine only three tangential components of the strain tensor. This is not enough to determine the six components of the strain tensor, which are generally present on the surface of the structure. In [14], we described a new model of piezoelectric sensor that measures bending strains on the surface of the structure. This sensor has a layered structure.

It is important to note that in a static electroelastic state, an electric charge appears on the sensor electrodes at the moment of application of a static load, but its value decreases very quickly to zero as a result of the appearance of an electric current in the electrical circuit connecting the electrodes and the influence of air ions. That is why the piezoelectric sensor is used only to measure dynamic deformations.

The error assessment of the sensor measurements and the choice of the sensor length depend on the geometry of the structure, the frequency of its oscillations, and the properties of the materials of the structure. In this paper, we will provide complete recommendations after a complex study of the mathematical model of the contact problem and a series of experiments.

In the model of the new piezoelectric sensor of bending strains, piezoelectric stacks are used as piezoelectric elements. These are layered elements of a periodic structure, which are produced industrially. Piezoelectric stacks are usually used as actuators. Piezoelectric stack actuators are a type of smart device that can activate large power and displacement outputs due to their unique stack configuration. They have been widely used in various engineering applications. As shown in the paper, the use of stacks in the sensor allows us to increase the magnitude of the electrical signal of the sensor and reduce its fragility.

The problem of calculating the effective moduli of inhomogeneous media with a periodic structure was posed at the beginning of the twentieth century in the papers of Poisson, Maxwell, Rayleigh, Voight W. [15], Reuss A. [16], and others. Voight W. used the values of the stiffness tensor, averaged by volume and orientation, as the effective moduli, and Reuss A. used the values of the inverse compliance tensor. Voight W. and Reuss A. made simple assumptions, without mathematical justification and error assessment, without studying the applicability area of simplified theories. In the second half of the 20th century, in numerous papers (see, for example, [17,18]) it was proved, using mathematical methods of the theory of functions of complex variables as well as asymptotic methods, that the Voight W. method gives an upper estimate and the Reuss A. method gives a lower estimate of the effective moduli. The difference between the results of these methods can reach very large values. Thus, for composites with very different characteristics, the error value of the Voight W. and Reuss A. approximations may be comparable to the effective moduli themselves and can exceed 100%.

Mathematical methods allow us to obtain justified formulas for effective characteristics of piezoelectric stacks.

To simplify the presentation of this new topic, we have neglected the influence of temperature and magnetic phenomena. In subsequent studies, we intend to consider the effect of temperature on the sensor operation. For this purpose, we will replace the equations of electroelasticity with the equations of thermoelectroelasticity.

We also did not consider the effect of humidity on the operation of the piezoelectric sensor. If the structures are tested at high humidity and for a long time, the sensors, as a rule, should be protected from moisture. Moisture penetrates the sensor materials and worsens their mechanical and electrical characteristics. These issues have been well studied and methods for sealing the sensors have been developed. To seal the sensors, various moisture-proof coatings are used, for example, several layers of moisture-resistant adhesives or layers based on bitumen, wax, rosin, or epoxy resins can be applied.

In the theory of strain sensors, it is assumed that the conditions of ideal contact exist in the contact area between the sensor and the structure. In practice, various methods for installing sensors can be used, for example, gluing or welding them to the surface of the structure. In the experiments described in [14], the sensors were glued.

Experimenters often must solve the following problem: at what points in the structure are the maximum stresses or displacements expected to occur, so that sensors can be placed there. Typically, the location of large stresses and displacements coincides with the lines of geometry distortion, areas of maximum load application, areas adjacent to rigid edge fastenings, and areas of contact between various structural elements. It is in these dangerous places that sensors should be placed.

## 2. Schematic Representations of Piezoelectric Stack and Basic Equations

In this section, we derive effective moduli for the piezoelectric composite active elements (stack) of a periodic structure [19]. The stack constitutes a layered bar obtained by sintering thin plates of piezoelectric ceramics with a strong piezoelectric effect and metal layers (electrodes). Piezoelectric ceramic plates are pre-polarized along the axis of the bar. Vanadium, copper, silver, aluminum, and platinum are used for the electrodes. The composite bar with a periodic structure is schematically depicted in Figure 1a. Piezoelectric layers are shown in white, while metal electrodes are shown in black. One cell consisting of one piezoelectric layer and one metal electrode is shown in Figure 1b.

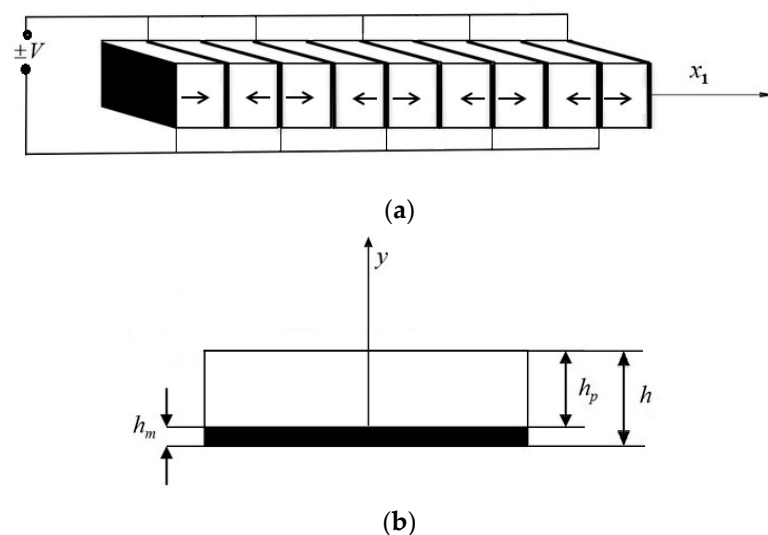


**Figure 1.** (a) Schematic structure of stack; (b) its periodic cell.

Figure 2 shows a sensor consisting of two external piezoelectric stacks and one middle elastic layer, which is shaded. In Figure 2, the wires connecting the electrodes and going to the voltmeter are marked in red. The conditions of ideal contact are met between all layers of the sensor. In Figure 2, the elastic layer and stacks are separated for clarity.

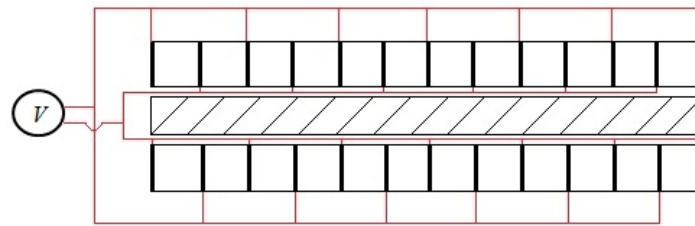


**Figure 2.** Schematic representation of a sensor with piezoelectric stack.

Figure 1a shows a piezoelectric stack, which has a periodic structure developed according to modern technology standards and is made by sintering piezoelectric layers with metal layers. Stacks of this type are industrially produced and are described in [19]. Figure 1b shows a periodicity cell for the stack shown in Figure 1a. The cell consists of two layers: one is a piezoelectric layer (marked in white in the figure) and the other a metal layer (marked in black in the figure). The condition of ideal contact is met between the layers. Figure 2 shows the design of a piezoelectric bending strain sensor. The sensor consists of two piezoelectric stacks, which are the outer layers of the sensor, ideally contacting the inner layer (marked in hatching in the figure). To show how the electrodes are connected, the distance between the inner layer of the sensor and the piezoelectric stacks is added in Figure 2. To illustrate the arrangement of the electrodes, Figure 2 shows conditionally the distance between the inner layer of the sensor and the piezoelectric stacks. In fact, the sensor design does not have this distance, and the condition of ideal contact is met.

Effective modules describe the physical properties of materials of a periodic structure. Their values do not depend on either the type of dynamic load or the edge conditions; therefore, when deriving formulas for effective modules, for simplicity, we take a dynamic load varying in time  $t$  as  $e^{-i\omega t}$ ; here,  $\omega$  is the circular oscillation frequency. This type of load makes it possible to further simplify the equations as a result of the transition to the amplitude values of the initial values.

Let us write out the well-known one-dimensional equations of elasticity and electroelasticity obtained using Kirchhoff hypotheses for mechanical quantities and the hypotheses formulated in [20] for the electric unknown quantities.

Equation of motion:

$$\frac{d\sigma_1}{dx_1} + \rho_d \omega^2 u_1 = 0 \quad (1)$$

where the subscript  $d$  at the letter  $\rho$  should be replaced by  $m$  for the metal layer and by  $p$  for the piezoelectric layer.

Hooke's law for a metal layer reads:

$$\sigma_1 = E_m e_1 \quad (2)$$

Electroelasticity relationship for a piezoceramic layer pre-polarized in the direction of the axis  $x_1$  is given by:

$$\sigma_1 = \frac{1}{s_{33}^E} e_1 - \frac{d_{33}}{s_{33}^E} E_1 \quad (3)$$

Electrostatic equations can be written as follows:

$$D_1 = s_{33}^E E_1 + d_{33} \sigma_1 E_1 = -\frac{d\varphi}{dx_1} \quad (4)$$

It is known that the magnitude of the electric potential at each electrode is a constant value:

$$\varphi|_{x=x_k \pm h_p/2} = \pm V \quad (5)$$

Here,  $x_k$  are the coordinates of the electrodes of the  $k$ -th layer. The relation between deformation and displacement has the form:

$$e_1 = \frac{du_1}{dx_1} \quad (6)$$

The symbols and terminology employed here align with those established earlier [20]. In Equations (1)–(6),  $E_1$  and  $D_1$  denote components of the electric field vector and the electric displacement vector along the  $x_1$  direction, respectively,  $s_{33}^E$  presents the elastic compliance at zero electric field,  $d_{33}$  is the piezoelectric constant,  $\epsilon_{33}^E$  is the dielectric constant at zero voltage, and  $\varphi$  is the electric potential.

To derive the effective moduli, we use the homogenization method [17,18]. The homogenization method, developed by famous mathematicians in the last century, allows us to obtain mathematically sound effective modules, the correctness of which is confirmed by mechanical experiments and practice. Since the designs and materials of the periodic structure are widely used, at the end of the twentieth century, the method aroused great interest among scientists and engineers. Unfortunately, nowadays the method is not often used. That is why we describe, in detail, the application of the homogenization method using a simple example, although other similar examples were considered earlier.

In the homogenization method, the electroelastic state in a periodic structure depends on both macroscopic and microscopic variables, the latter being defined within the periodic cell. For simplicity, macroscopic variables are denoted by  $x$ .

We introduce the following scaling on a single cell:

$$y = x/\varepsilon, \varepsilon = h/l, h = h_m + h_p \quad (7)$$

Then:

$$\frac{d}{dx} = \frac{\partial}{\partial x} + \varepsilon^{-1} \frac{\partial}{\partial y} \quad (8)$$

The sought quantities that determine the behavior of a one-dimensional layered periodic structure can be expressed as asymptotic expansions in a small parameter  $\varepsilon$ :

$$F(x) = F^0(x,y) + \varepsilon F^1(x,y) + \varepsilon^2 F^2(x,y) + \dots \quad (9)$$

The superscript of the function  $F^i(x)$  is equal to the degree  $\varepsilon^i$  in the term on the right side of the Formula (9) and means the approximation number.

The derivative of the function  $F(x)$ , taking into account Formula (9), can be written as:

$$\frac{dF(x)}{dx} = \frac{\partial F^0(x,y)}{\partial x} + \frac{1}{\varepsilon} \frac{\partial F^0(x,y)}{\partial y} + \varepsilon \frac{\partial F^1(x,y)}{\partial y} + \varepsilon^2 \frac{\partial F^2(x,y)}{\partial x} + \varepsilon \frac{\partial F^2(x,y)}{\partial y} + \dots \quad (10)$$

$F(x)$  refers to any of the required quantities—displacement, stress, deformation, electrical quantities. All functions  $F^i(x,y)$  are smooth in  $y$  and periodic in  $y$ , equal in magnitude and opposite in sign on opposite sides of the cell. Let us imagine the desired quantities and their derivatives in the form of Equations (9) and (10), substitute these expansions into the original Equations (1)–(6), and put the coefficients at the same degrees of the small parameter  $\varepsilon$  equal to zero. As a result, we obtain the following equations:

Equations of motion:

$$\begin{aligned} \frac{\partial \sigma^0}{\partial y} &= 0, \frac{\partial \sigma^0}{\partial x} + \frac{\partial \sigma^1}{\partial y} + \rho_d \omega^2 u^0(x,y) = 0 \\ \frac{\partial \sigma^k}{\partial x} + \frac{\partial \sigma^{k+1}}{\partial y} + \rho_d \omega^2 u^k(x,y) &= 0, k = 1, 2, \dots \end{aligned} \quad (11)$$

From the first formula of (11), it follows that  $\sigma^0 = \sigma^0(x)$ , and this is accounted for in the second equation of (11).

Formulas linking displacement by strains are written as:

$$\frac{\partial u^0}{\partial y} = 0, e^0 = \frac{du^0}{dx} + \frac{du^1}{dy}, e^k = \frac{\partial u^k}{\partial x} + \frac{\partial u^{k+1}}{\partial y}, k = 1, 2, \dots \quad (12)$$

From the first formula of (12), it follows that  $u^0 = u^0(x)$ , and this is taken into account in the second formula of (12).

Equations of state for metal layers have the form:

$$\sigma^k = E_m e^k, k = 0, 1, 2, \dots \quad (13)$$

Relations of electroelasticity for piezoelectric layers can be written as:

$$\sigma^k = \frac{1}{s_{33}^E} e^k - \frac{d_{33}}{s_{33}^E} E_1^k, k = 0, 1, 2, \dots \quad (14)$$

Electrostatic equations are given by:

$$\varphi^0 = const, E_1^0 = -\frac{\partial \varphi^1}{\partial y}, E_1^k = -\frac{\partial \varphi^{k+1}}{\partial y}, k = 1, 2, \dots \quad (15)$$

In the piezoelectric layer,  $E_1^0$  is a constant value, and electrical potential  $\varphi$  is a linear function of argument  $y$ ; for the elastic layers, these values are absent. After satisfying the conditions (5) on the electrodes of the piezoelectric layer, the electric potential is  $\varphi = \varphi^0 + \varepsilon \varphi^1$  and electric field strength is  $E_1^0$ .

$$\varphi = V \left( 1 - \varepsilon \frac{2Y}{h_p} + \varepsilon \frac{2y}{h_p} \right), E_1^0 = -V \frac{2}{h}, Y = \frac{h}{\varepsilon} \quad (16)$$

### 3. Effective Moduli and Equations of the Macroscopic Electroelastic State for Stack

We now integrate, with respect to local variable  $y$ , Equations (13) and (14) in the interval of the periodicity of the cell, taking into account that the properties of the layer materials are piecewise continuous functions:

$$E_y = \begin{cases} E_m, & 0 \leq y \leq h_m/\varepsilon \\ 1/s_{33}^E, & h_m/\varepsilon \leq y \leq Y \end{cases}, d_{33y} = \begin{cases} 0, & 0 \leq y \leq h_m/\varepsilon \\ d_{33}, & h_m/\varepsilon \leq y \leq Y \end{cases} \quad (17)$$

$$\varepsilon_{33y}^T = \begin{cases} 0, & 0 \leq y \leq h_m/\varepsilon \\ \varepsilon_{33}^T, & h_m/\varepsilon \leq y \leq Y \end{cases}, Y = \frac{h_m + h_p}{\varepsilon}$$

Then, the ratio of electroelasticity for the cell is written as:

$$\sigma^0 = E_y (e^0 - d_{33y} E_1^0) \quad (18)$$

We divide this relation by  $E_y$  and integrate over  $y$  within the periodicity of the cell from 0 to  $Y$ . As a result, we obtain the averaged ratio of electroelasticity:

$$\sigma^0 = \tilde{E} (e^0 - \tilde{d}_{33} E_1^0), D_1^0 = \tilde{s}_{33}^T E_1^0 + \tilde{d}_{33} \sigma^0 \quad (19)$$

$$\tilde{E} = h / (h_p s_{33}^E + h_m / E_m), \tilde{d}_{33} = d_{33} h_p / h, \tilde{s}_{33}^T = s_{33}^T h_p / h$$

Here, magnitudes with a wave form above  $\tilde{E}$ ,  $\tilde{d}_{33}$ , and  $\tilde{s}_{33}^T$  are the effective moduli.

Similarly, integrating the second equation of (11) within the periodicity cell, we obtain the averaged equation of motion:

$$\frac{d\sigma^0}{dx} + \omega^2 \tilde{\rho} u^0 = 0, \tilde{\rho} = \frac{h_p \rho_p + h_m \rho_m}{h} \quad (20)$$

where  $\tilde{\rho}$  is the material density averaged within the cell.

Integrating the second formula of (12) within the periodic cell, we obtain the relation as in the theory of isotropic bars:

$$e^0 = \frac{du^0}{dx} \quad (21)$$

Here, it is taken into account that the integrals with respect to  $y$  of periodic functions  $\partial\sigma^1(x,y)/\partial y$  are equal to zero.

Equations (19)–(21) constitute a complete system of equations describing the macroscopic behavior of the bar. They differ from the corresponding equations of the theory of isotropic bars only in the sense of physical constants.

There is no need to derive a rapidly changing electroelastic state, since it is not required in the theory of the sensor.

#### 4. Analysis of Effective Moduli of Piezoelectric Stacks

A very important characteristic of the performance of piezoelectric elements is the electromechanical coupling coefficient (EMCC). It gives the ratio of the electrical (mechanical) energy stored in the volume of a piezoelectric stack and is capable of converting to the total mechanical (electrical) energy supplied to the stack. Generally speaking, determination of EMCC is a difficult problem.

To evaluate EMCC, we will need an effective coupling coefficient formula for the effective coupling coefficient  $\tilde{k}_{33}$ :

$$\tilde{k}_{33}^2 = \frac{\tilde{d}_{33}^2 \tilde{E}}{\tilde{\epsilon}_{33}} \quad (22)$$

We have calculated and plotted the dependence of the effective characteristics of a stack with PZT-8 piezoelectric ceramics [21] on the thickness of the electrode layer in the stack. Figure 3 shows this dependence for the copper electrodes and Figure 4 shows similar results for the silver electrodes.

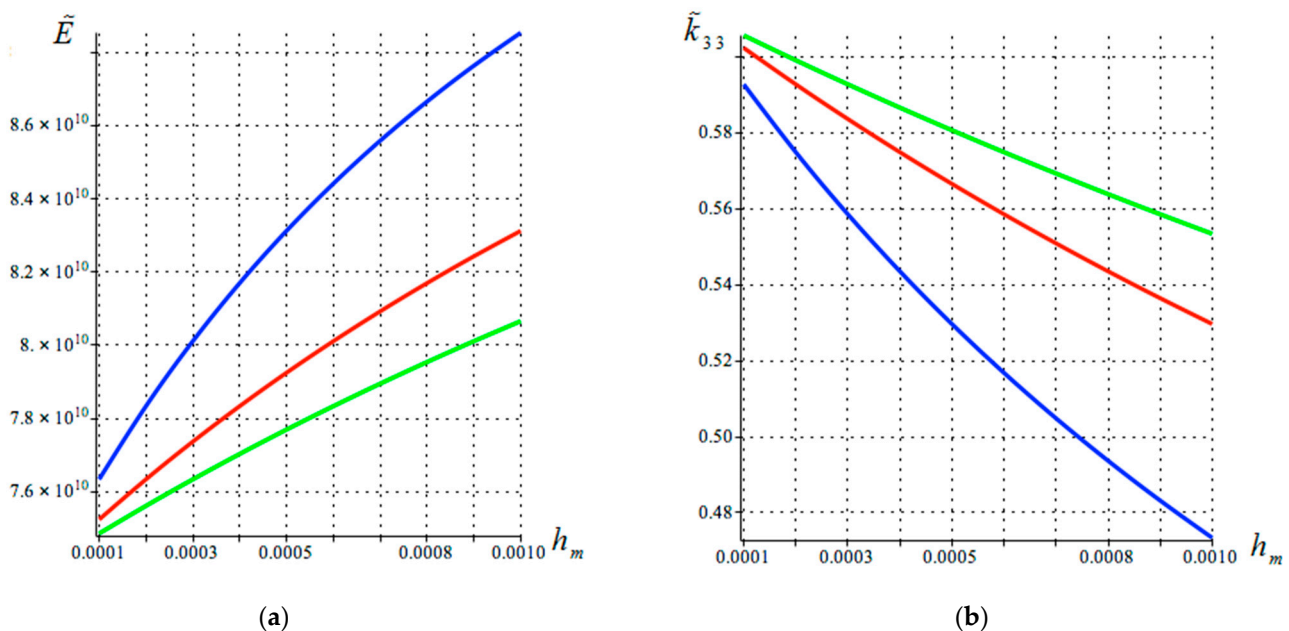


**Figure 3.** Dependence of (a) effective elastic modulus (N/m<sup>2</sup>) and (b) effective EMCC (a dimensionless quantity) on the thickness copper electrode layer  $h_m$  (m).

In Figure 3, the blue line corresponds to the thickness of the piezoelectric layer  $h_p = 0.001$  m; the red line corresponds to the thickness of the piezoelectric layer  $h_p = 0.002$  m; and the green line corresponds to the thickness of the piezoelectric layer  $h_p = 0.003$  m.

The plots in Figure 3 show that the effective elastic modulus of the stack increases with increasing metal layers, since the elastic modulus of the copper is greater than the elastic modulus of the piezoelectric ceramics. The EMCC decreases with the increasing thickness of the metal layer.

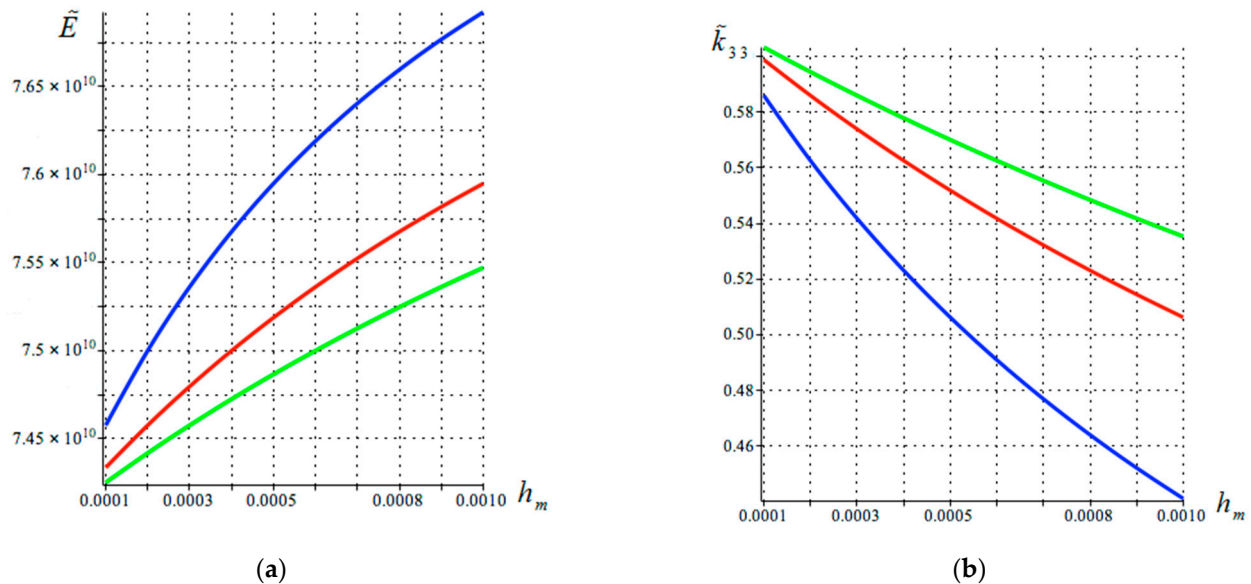


**Figure 4.** Dependence of (a) effective elastic modulus (N/m<sup>2</sup>) and (b) effective EMCC (a dimensionless quantity) on the silver electrode layer thickness  $h_m$  (m).

The value of the elastic modulus of silver is closer to the elastic modulus of piezoelectric ceramics PZT-8 than the value of the elastic modulus of copper. Therefore, the influence on the effective elastic modulus and effective EMCC in the case of silver electrodes will be less pronounced than in the case of copper electrodes.

Let us consider another type of stack [20], the cell of which consists of a piezoceramic layer, the surfaces of which are covered with metal electrodes and an adhesive layer. Electrodes, as a rule, are applied to piezoelectric layers by spraying. The thickness of the electrode is significantly less than the thicknesses of the piezoelectric and the adhesive layers, so the electrodes can be ignored when calculating the effective moduli. The derivation of effective moduli for such a stack completely repeats the derivation for the first type of stack. In this case, formulas for effective moduli can be obtained by replacing the lower indices  $m$  with  $a$  in (17). In this case, the dependence of the effective moduli of elasticity and the effective EMCC on the adhesive layer thickness is shown in Figure 5.

In Figures 3–5, the blue line corresponds to the thickness of the piezoelectric layer  $h_p = 0.001$  m; the red line corresponds to the thickness of the piezoelectric layer  $h_p = 0.002$  m; and the green line corresponds to the thickness of the piezoelectric layer  $h_p = 0.003$  m.

Figure 5 shows how both the effective modulus of elasticity and EMCC decrease with the increasing thickness of the adhesive layer. Since the elastic modulus of the adhesive is significantly smaller than the elastic modulus of the piezoelectric ceramics, the presence of adhesive layers in the stack significantly reduces the effective elastic modulus and effective EMCC.

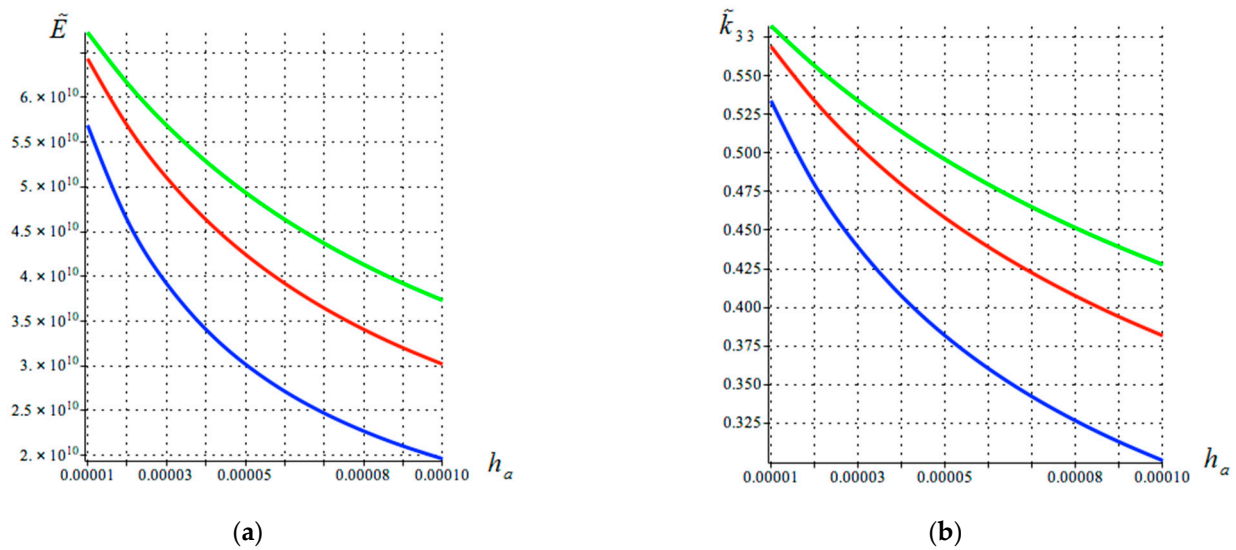


**Figure 5.** Dependence of (a) effective elastic modulus (N/m<sup>2</sup>) and (b) effective EMCC (a dimensionless quantity) on the adhesive layer thickness  $h_a$  (m).

### 5. Electromechanical Coupling Coefficient (EMCC)

The most important property of piezoelectric materials is their ability to convert energy: mechanical energy into electrical energy and vice versa. The electromechanical coupling coefficient (EMCC) is widely used to evaluate the efficiency of energy conversion. The generally accepted and understandable definition of EMCC is formulated as follows: EMCC is the ratio of the energy capable of conversion to the total energy stored in the deformed body. However, there is no single answer to how to find the energy that can be converted. The definition of EMCC was studied deeply in the second half of the 20th century. Unfortunately, interest in the definition of EMCC has decreased recently. That is why we will describe the derivation of the formula for calculating the EMCC, using the results found in [22]. In our previous work [14], EMCC was calculated for a simple piezoelectric bending strain sensor, and it was shown that it depends on the sensor parameters. For a new piezoelectric sensor with increased efficiency and improved strength, the derivation of the formula for EMCC is similar to that presented in the article [14]. Since the effective properties of stacks are different from the properties of piezoelectric plates [14], we will derive the formula for determining EMCC for our new high efficiency and strength bending strain sensor.

In [22], a study of various methods for calculating EMCC was conducted. One of the most common formulas for calculating EMCC is written as follows:

$$k_s^2 = \frac{U_m^2}{U_e U_d} \quad (23)$$

where  $U_e$ ,  $U_d$ , and  $U_m$  are the elastic, electric, and interaction energy, respectively. The EMCC in Equation (23) is designated as  $k_s^2$ .

The results of article [22] prove that Equation (23) is applicable only for electroelastic states as uniform states, and it is not suitable for electroelastic states changing in coordinates and time. According to this formula, it is possible to determine only the tabular characteristics of the piezoelectric material  $k_{33}$ ,  $k_{31}$ , etc.

The second method for determining EMCC belongs to Mason. In Mason's formula, the resonant and antiresonant frequencies of vibrations of the piezoelectric element are used to calculate EMCC:

$$k_d^2 = \frac{\omega_a^2 - \omega_r^2}{\omega_a^2} \quad (24)$$

where  $\omega_r$  is the resonance frequency of the vibrations and  $\omega_a$  is the corresponding antiresonance frequency of the vibrations.

Note that Equation (24) gives the EMCC, denoted here as  $k_d^2$ , for one vibration frequency  $\omega$ , contained in the interval from  $(\omega_r, \omega_a)$ . It gives the values of EMCC for individual specific values of the circular frequency  $\omega$ . Due to its simplicity, Equation (24) is often used in modern papers [23–27].

The most general formula for calculating EMCC is the following [22]:

$$k_e^2 = \frac{U^{(d)} - U^{(sh)}}{U^{(d)}} \quad (25)$$

Here and in the future, the values with the upper indices (*sh*) and (*d*) refer to problems with short-closed and open electrodes, respectively. In this way,  $U^{(d)}$  is the internal energy of the piezoelectric element with disconnected electrodes and  $U^{(sh)}$  is the internal energy for the element with short-circuited electrodes.

In [22], it is shown that this equation is applicable to any problem of statics and dynamics. Note that the calculation of EMCC  $k_e$  is a complex problem. To determine  $k_e$ , three problems must be solved. The first problem is to determine the electroelastic state of the original problem. In the second problem, we calculate the internal energy of the piezoelectric element with disconnected electrodes  $U^{(d)}$ . The condition on open electrodes is written as:

$$\int_S D_3^{(d)} ds = 0 \quad (26)$$

where  $s$  is the surface of the electrode and  $D_3^{(d)}$  is the component of elastic induction vector normal to the electrode surface.

In the third problem, the internal energy for a piezoelectric element with short-circuited electrodes must be determined. When solving the second and third problems, it is assumed that the deformations from the original problem are known.

For the conditions of short-circuited electrodes, the electric potential  $\varphi^{(sh)}$  must be zero:

$$\varphi^{(sh)} = 0 \quad (27)$$

Note that the equation for calculating the EMCC (25) is applicable for any problem. The energy method of determining the EMCC was discussed previously in [22]. In the case of a uniform state, the values of  $k_e$  coincide with the values of  $k_s$ ; near resonances  $k_e$  coincides with  $k_d$ .

We will use Equation (25) for our new high efficiency and strength bending strains sensor. The equations for the stacks use the effective coefficients found above. Below are the equations for the first type of stacks obtained by sintering.

Electric current in the case of vibrations with a circular frequency  $\omega$  is calculated by the following equation:

$$I = -i\omega \int_{\Omega} D_{3,0} d\Omega = -i\omega \Omega \left[ -\frac{2V}{h_2} \tilde{\varepsilon}_{33}^T (1 - \tilde{k}_{33}^2) + (z_2 + z_1) \frac{\tilde{\varepsilon}_{33}^T \tilde{k}_{33}^2}{2\tilde{d}_{33}l} \frac{dw_0}{d\xi} \Big|_{\xi=1} + \frac{\tilde{d}_{33}}{\tilde{s}_{33}^T} u_0 \Big|_{\xi=1} \right] \quad (28)$$

Since the quantities  $U^{(d)}$  and  $U^{(sh)}$  are even functions of the variable  $x_3$ , we will calculate  $U^{(d)}$  and  $U^{(sh)}$  only for the values  $x_3 \geq 0$ . The superscripts ( $\pm$ ) should be omitted from the equations.

In the case of open electrodes, the following equations hold true:

$$\begin{aligned} D_{3,0}^{(d)} &= 0, E_{3,0}^{(d)} = -\frac{2V^{(d)}}{h_p} + (h + h_e) \frac{\tilde{k}_{33}^2}{2(1-\tilde{k}_{33}^2)} \frac{1}{d_{33}} e_{1,1} = 0, \\ V^{(d)} &= (h + h_e) h_p \frac{\tilde{k}_{33}^2}{4(1-\tilde{k}_{33}^2)} \frac{1}{d_{33}} e_{1,1}, E_{3,1}^{(d)} = -\frac{\tilde{k}_{33}^2}{1-\tilde{k}_{33}^2} \frac{1}{d_{33}} e_{1,1}, \\ \sigma_{1,1}^{(d)} &= -\frac{1}{\tilde{s}_{33}^T} \frac{1}{1-\tilde{k}_{33}^2} e_{1,1}, \sigma_{1,0}^{(d)} = 0. \end{aligned} \quad (29)$$

For the case of short-circuited electrodes, the following equations apply:

$$\begin{aligned} V^{(sh)} &= 0, E_{3,0}^{(sh)} = (h + h_e) \frac{\tilde{k}_{33}^2}{2(1-\tilde{k}_{33}^2)} \frac{1}{d_{33}} e_{1,1}, D_{3,0}^{(sh)} = (h + h_e) \frac{\tilde{k}_{33}^2}{2} \frac{\tilde{\epsilon}_{33}^T}{d_{33}} e_{1,1}, \\ E_{3,1}^{(sh)} &= -\frac{\tilde{k}_{33}^2}{1-\tilde{k}_{33}^2} \frac{1}{d_{33}} e_{1,1}, \sigma_{1,1}^{(sh)} = \frac{1}{\tilde{s}_{33}^T} \frac{1}{1-\tilde{k}_{33}^2} e_{1,1}, \\ \sigma_{1,0}^{(sh)} &= -(h + h_e) \frac{\tilde{k}_{33}^2}{2(1-\tilde{k}_{33}^2)} \frac{1}{\tilde{s}_{33}^T} e_{1,1} \end{aligned} \quad (30)$$

Using Equations (29) and (30), obtained above, we present the expressions for the internal energy of the sensor with open electrodes  $U^{(d)}$  and its internal energy in the case of short-circuited electrodes  $U^{(sh)}$ :

$$\begin{aligned} U^{(d)} &= \int_V \gamma \sigma_1^{(1)(d)} \gamma e_1^{(1)} dv + U^{(e)} = \frac{(h^3 - h_e^3)}{3(1-k^2)} \frac{e_1^{(1)2}}{\tilde{s}_{33}^T} + U^{(e)} \\ U^{(e)} &= \int_V \gamma \sigma_1^{(1)(e)} \gamma e_1^{(1)} dv = \frac{h_e^3}{3} E e_1^{(1)2} \end{aligned} \quad (31)$$

$$\begin{aligned} U^{(sh)} &= \int_V \left[ \left( \sigma_1^{(0)(sh)} + \gamma \sigma_1^{(1)(sh)} \right) \gamma e_1^{(1)} + \left( E_3^{(0)(sh)} + \gamma E_3^{(1)(sh)} \right) D_3^{(0)(sh)} \right] dv + U^{(e)} \\ &= \frac{1}{1-k^2} \frac{e_1^{(1)2}}{\tilde{s}_{33}^T} \left( -\frac{(h^2 - h_e^2)(h + h_e)k^2}{2} + \frac{h^3 - h_e^3}{3} + h_p \frac{(h + h_e)^2 k^2}{4} \right) + U^{(e)} \\ &= \frac{1}{1-k^2} \frac{e_1^{(1)2}}{\tilde{s}_{33}^T} \left( -h_p \frac{(h + h_e)^2 k^2}{4} + \frac{h^3 - h_e^3}{3} \right) + U^{(e)} \end{aligned} \quad (32)$$

Finally, the EMCC  $k_e$  can be evaluated using Equation (25)

$$\tilde{k}_e^2 = \frac{U^{(d)} - U^{(sh)}}{U^{(d)}} = \frac{3\tilde{k}_{33}^2}{4} \frac{h_p(h + h_e)^2}{h^3 + h_e^3(E\tilde{s}_{33}^T - 1)} \quad (33)$$

Using Equation (33), we calculate EMCC for the new high efficiency and strength bending strain sensor.

## 6. Equations for Calculating Bending Deformation Based on the Experimentally Measured Difference in Electric Potential on the Sensor Electrodes

In our previous paper [14], for a classic bending strain sensor, a detailed derivation of the equations for calculating the strain from the measured electrical signal and EMCC is given. The derivation of the main results for the modified sensor is performed in exactly the same way here. The equations for the sensor of the first type (the stacks of this sensor are obtained by sintering piezoelectric ceramics with metal electrodes) are written out by analogy, replacing the physical constants in the formulas of the paper [14] with corresponding effective moduli. The bending deformations  $\kappa$  for an arbitrary dependence

of the stress-strain state of a body on time can be determined in accordance with the follow equation:

$$\frac{d\kappa}{dt} = \frac{2\tilde{d}_{33}}{\tilde{k}_{33}^2(h+h_m)} \left( \frac{VY}{\tilde{\varepsilon}_{33}^T \Omega} + \frac{2}{h_p} \frac{dV}{dt} (1 - \tilde{k}_{33}^2) \right) \quad (34)$$

In the case of harmonic vibrations of a deformable body according to the law  $e^{-i\omega t}$  ( $\omega$  is the circular frequency of vibrations), Equation (23) takes a simpler form:

$$\kappa = \frac{2V}{h_p} \frac{\tilde{d}_{33}}{\tilde{k}_{33}^2(h+h_m)} \left( i \frac{Yh_p}{\tilde{\varepsilon}_{33}^T \omega \Omega \tilde{k}_{33}^2} + \frac{2(1 - \tilde{k}_{33}^2)}{\tilde{k}_{33}^2} \right) \quad (35)$$

All quantities on the right-hand sides of Equations (34) and (35) are known. Therefore, using the difference in electric potential  $V$  measured by the voltmeter on the sensor electrodes, we can calculate the bending deformation component  $k$  using Equations (34) or (35).

One of the characteristics of Lord Kelvin strain gauges is the sensitivity coefficient, which is defined as the ratio of the relative change in the resistance of the sensor conductor to the relative deformation of the sensor (the sensor is considered as a one-dimensional element). Note that the sensitivity of the Lord Kelvin sensor is a small value.

The sensor proposed in the article is an effective energy converter, so we will consider the EMCC as a measure of its sensitivity. The EMCC shows what amount of mechanical energy of the sensor, as a result of sensor deformation, is converted into electrical energy as a result of the direct piezoelectric effect. For a sensor based on the use of piezoelectric stacks, the sensitivity exceeds 0.5 (50%).

## 7. Determination of Bending Components of Deformations at a Point on the Surface of a Structure Based on Sensor Socket Readings

The bending deformations on the surface of the structure being studied are described by three strain components: tensor,  $\kappa_{xx}$ , and  $\tau_{xy}$ . Torsional deformations cannot be measured by a sensor, since sensors only measure  $\kappa_{xx}$  and  $\kappa_{yy}$  and do not respond to torsional deformations.

In this case, proceed as follows: at a point on the body, measure deformations  $\kappa_A$ ,  $\kappa_B$ , and  $\kappa_C$  in three directions at angles  $\beta_A$ ,  $\beta_B$ , and  $\beta_C$  relative to the  $x$ -axis (Figure 6).

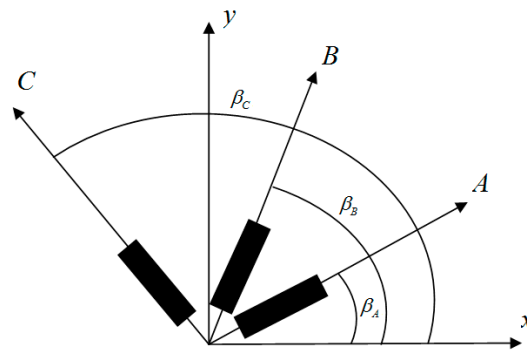


**Figure 6.** Three sensors located at arbitrary angles relative to the  $x$ -axis.

The equations for transforming deformations when rotating coordinate axes have the familiar form:

$$\begin{aligned} \kappa_A &= \kappa_{xx} \cos^2 \beta_A + \kappa_{yy} \sin^2 \beta_A + \tau_{xy} \sin \beta_A \cos \beta_A, \\ \kappa_B &= \kappa_{xx} \cos^2 \beta_B + \kappa_{yy} \sin^2 \beta_B + \tau_{xy} \sin \beta_B \cos \beta_B, \\ \kappa_C &= \kappa_{xx} \cos^2 \beta_C + \kappa_{yy} \sin^2 \beta_C + \tau_{xy} \sin \beta_C \cos \beta_C. \end{aligned} \quad (36)$$

For given angles  $\beta_A$ ,  $\beta_B$ , and  $\beta_C$ , and known results of strain measurements  $\kappa_A$ ,  $\kappa_B$ , and  $\kappa_C$ , components of the strain tensor in the Cartesian coordinate system ( $\kappa_{xx}$ ,  $\kappa_{yy}$ , and  $\tau_{xy}$ ) are found by solving the system of Equation (30).

To determine the torsional deformation, the following equation is used:

$$\gamma_{xy} = 2\kappa_B - \kappa_A - \kappa_C \quad (37)$$

The principal deformations  $\kappa_1$  and  $\kappa_2$ , as well as their directions, are calculated using the following equation:

$$\begin{aligned} \kappa_1 &= \frac{1}{2}(\kappa_{xx} + \kappa_{yy}) + \frac{1}{2}\sqrt{(\kappa_{xx} - \kappa_{yy})^2 + \tau_{xy}^2}, \\ \kappa_2 &= \frac{1}{2}(\kappa_{xx} + \kappa_{yy}) - \frac{1}{2}\sqrt{(\kappa_{xx} - \kappa_{yy})^2 + \tau_{xy}^2}, \\ 2\beta &= \arctg\left(\frac{\tau_{xy}}{(\kappa_{xx} - \kappa_{yy})}\right). \end{aligned} \quad (38)$$

where  $\beta$  is the angle of inclination of the strain  $\kappa_1$  to the axis  $x$ .

Based on the main values of deformation  $\kappa_1$  and  $\kappa_2$ , we determine the stress on the surface and the maximum torsional stress at the point:

$$\sigma_1 = \frac{E}{1-\nu^2}(\kappa_1 + \nu\kappa_2), \quad \sigma_2 = \frac{E}{1-\nu^2}(\kappa_2 + \nu\kappa_1), \quad \tau_{\max} = \frac{\sigma_1 - \sigma_2}{2}, \quad (39)$$

where  $E$  is the elastic modulus and  $\nu$  is Poisson's ratio.

The most commonly used arrangement of strain gauges is in the form of a delta socket (Figure 7).

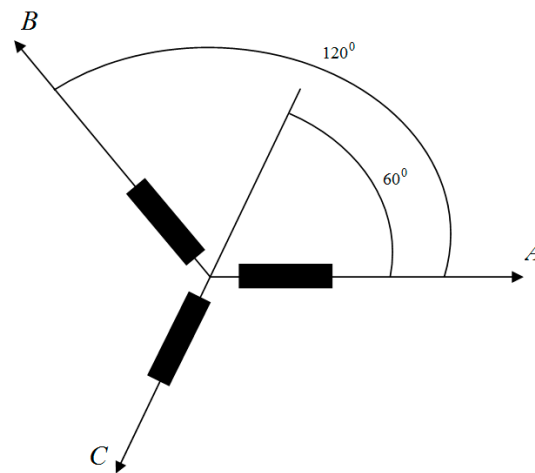


Figure 7. Delta socket.

For a delta socket, the sensor directions are characterized by the following angles:  $\beta_A = 0$ ,  $\beta_B = 60^\circ$ , and  $\beta_C = 120^\circ$ .

The main deformations  $\kappa_1$  and  $\kappa_2$  and their orientation relative to the  $x$ -axis and angle  $\beta$  are determined in accordance with the following equation:

$$\begin{aligned} \kappa_1 &= \frac{\kappa_A + \kappa_B + \kappa_C}{3} + \sqrt{\left(\kappa_A - \frac{\kappa_A + \kappa_B + \kappa_C}{3}\right)^2 + \left(\frac{\kappa_B - \kappa_C}{\sqrt{3}}\right)^2}, \\ \kappa_2 &= \frac{\kappa_A + \kappa_B + \kappa_C}{3} - \sqrt{\left(\kappa_A - \frac{\kappa_A + \kappa_B + \kappa_C}{3}\right)^2 + \left(\frac{\kappa_B - \kappa_C}{\sqrt{3}}\right)^2}, \\ \beta &= \arctg \frac{(\kappa_B - \kappa_C)/\sqrt{3}}{\kappa_A - (\kappa_A + \kappa_B + \kappa_C)/3}. \end{aligned} \quad (40)$$

Torsional voltages for the delta socket through sensor readings  $\kappa_A$ ,  $\kappa_B$ , and  $\kappa_C$  are determined by the following equations:

$$\begin{aligned}\sigma_1 &= E \left[ \frac{\kappa_A + \kappa_B + \kappa_C}{3(1-\nu)} + \frac{1}{1+\nu} \sqrt{\left( \kappa_A - \frac{\kappa_A + \kappa_B + \kappa_C}{3} \right)^2 + \left( \frac{\kappa_B - \kappa_C}{\sqrt{3}} \right)^2} \right], \\ \sigma_2 &= E \left[ \frac{\kappa_A + \kappa_B + \kappa_C}{3(1-\nu)} - \frac{1}{1+\nu} \sqrt{\left( \kappa_A - \frac{\kappa_A + \kappa_B + \kappa_C}{3} \right)^2 + \left( \frac{\kappa_B - \kappa_C}{\sqrt{3}} \right)^2} \right]\end{aligned}\quad (41)$$

## 8. Conclusions

This paper builds a mathematically sound model of a new modified piezoelectric sensor of bending deformations. The new sensor uses the best energy converters of the present time—piezoelectric stacks. Piezoelectric stacks have been applied in a large variety of domains, including optoelectronics, aerospace science and technology, MEDTEC, precision metrology, etc. [19,23–30]. The advantages of piezoelectric stacks are their: fast response, high acceleration rates, high power generation, compact design, high mechanical power density, and low power consumption.

Stacks are usually used as actuators. We have applied them in strain sensors.

Using piezoelectric sensors to determine strain is very simple: first, measure the electrical signal from the sensor electrodes (experiments are described in [14]), then calculate strains based on the measured electrical signal. For example, for a modified sensor of type 1, bending strains should be determined using Equations (34) and (35). It is very important to have the correct equations to calculate strains. If the equations are incorrect or the effective moduli are obtained incorrectly, strains will be determined incorrectly, and the results of the experiment will be erroneous. We use modern mathematics to obtain the correct effective moduli and Equations (34) and (35).

Bending strains can be experimentally determined not only by new piezoelectric sensors of bending strains, but also by other experimental methods. Let us discuss the advantages of piezoelectric sensors compared to the following methods of determining bending strains:

- brittle strain-sensitive coatings: deformations are determined by the formation of cracks during deformation.
- The Moire fringe method (Moire method) is based on the occurrence of interference fringes, which are geometric locations of equal displacements. The method uses dividing Moire images, recorded either by photogrammetry or by digital recording. The grid is deformed together with the body under study, and measurements are carried out using a microscope.
- Optically sensitive coatings: measurements are carried out only on the surface accessible for observation. Coatings are made of transparent, optically sensitive material 1–3 mm thick.
- Holographic interferometry using a laser allows measuring displacements in three-dimensional structures. The method is applicable for precise measurements of small displacements of surface points under mechanical, thermal, and other loads, for studying vibrations of objects and recording structural changes in materials during mechanical testing.
- Polarization: the optical method allows finding strain and stress fields for objects made of transparent materials.

With all their advantages—a well-developed theoretical basis, with good measurement accuracy—these methods of measuring bending deformations are not suitable for long-term observations, since they require additional equipment, and the results of their measurements require complex processing with the personal participation of a specialist and only allow determining the desired values at one fixed point in time. For example, the use of brittle coatings allows you to find areas of destruction of the coating of the structure under high stresses or displacements only once; it is difficult to imagine a structure whose

stress-strain state is monitored for a long time by the holographic interferometry method using numerous lasers at different points of the structure; to use the polarization—optical method, the object under study must be made of a transparent material, etc.

In the case of a thin-walled structure, the change in curvature can be measured by placing two parallel sensors on the opposite structure's faces. These sensors should be positioned at points where the normal to the middle surface intersects the faces. The bending strain is calculated based on the difference in longitudinal strains recorded by the sensors. However, in practical scenarios, this approach is often difficult to implement. For example, it may be impossible to measure strains on the inner surface of a nuclear reactor or the outer surface of a dome covered with snow or ice, or even a waterproofing layer, etc.

Piezoelectric sensors are ideal for long-term observations of the stress-strain state of a structure, and there are no restrictions on the number of sensors used. Proof of the reliable operation of piezoelectric elements and especially piezoelectric stacks is their many years of operation in electronics, robotics, generators, actuators, and combined systems, from lighting technology to high-precision industrial systems, which confirms the status of piezoelectric material as one of the most promising materials of our time.

As is known, piezoelectric sensors are effective, easy to use, and cheap. Sensors that use piezoelectric stacks are significantly more expensive than sensors with simple piezoelectric elements. But sensors that use piezoelectric stacks have several excellent advantages, including increased efficiency and good strength properties. We especially recommend using them in important and responsible structures.

Let us note the special achievements of the article:

- to calculate the effective characteristics of piezoelectric stacks with a periodic structure, we applied a modern mathematical method—the averaging (homogenization) method;
- we replaced the piezoelectric plates in the first piezoelectric bending strain sensor [14] with piezoelectric stacks and received a new high efficiency and strength bending strain sensor;
- previously used tangential strain sensors, together with our new bending strain sensors, allow us to determine all components of the strain tensor at any point on the surface of the structure under study. Since piezoelectric sensors are simple and reliable to use and do not require additional energy sources, the properties of the sensor materials are stable, and they will fit perfectly into BIM construction technologies, both at the design stage and at the operation stage, at all stages of the life cycle of a construction site. In addition, they are indispensable in creating digital twins of construction site. The increased reliability of the proposed piezoelectric composite sensor with stacks, as well as the accuracy and stability of deformation measurements by such a sensor, ensures an increase in the mechanical safety of building structures due to an increase in the efficiency of their monitoring.

**Author Contributions:** V.S., N.R. and Y.Z. have contributed equally to the manuscript. All authors have read and agreed to the published version of the manuscript.

**Funding:** The research was funded by the National Research Moscow State University of Civil Engineering (grant for fundamental and applied scientific research, project No. 23-392/130).

**Data Availability Statement:** Data are contained within the article.

**Conflicts of Interest:** The authors declare no conflicts of interest.

## References

1. Toroń, B.; Szperlich, P.; Nowak, M.; Starczewska, A. A novel method for measuring piezoelectric coefficients. *Measurement* **2023**, *206*, 112274. [[CrossRef](#)]
2. Kamal, A.; Kulkarni, V.; Sahoo, N. Measurement of Strain Using Strain Gauge and Piezoelectric Sensors. In *Applications and Techniques for Experimental Stress Analysis*; IGI Global: Hershey, PA, USA, 2020; pp. 91–101. [[CrossRef](#)]
3. Kim, K.; Kim, J.; Jiang, X.; Kim, T. Static Force Measurement Using Piezoelectric Sensors. *J. Sens.* **2021**, *2021*, 6664200. [[CrossRef](#)]

4. Seethaler, R.; Mansour, S.Z.; Ruppert, M.G.; Fleming, A.J. Position and force sensing using strain gauges integrated into piezoelectric bender electrodes. *Sens. Actuators A Phys.* **2021**, *321*, 112416. [CrossRef]
5. Seethaler, R.; Mansour, S.Z.; Ruppert, M.G.; Fleming, A.J. Piezoelectric benders with strain sensing electrodes: Sensor design for position control and force estimation. *Sens. Actuators A Phys.* **2022**, *335*, 113384. [CrossRef]
6. Srinivasaraghavan Govindarajan, R.; Rojas-Nastrucci, E.; Kim, D. Surface Acoustic Wave-Based Flexible Piezocomposite Strain Sensor. *Crystals* **2021**, *11*, 1576. [CrossRef]
7. Suzuki, A.; Liao, W.; Shibata, D.; Yoshino, Y.; Kimura, Y.; Shimoi, N. Structural Damage Detection Technique of Secondary Building Components Using Piezoelectric Sensors. *Buildings* **2023**, *13*, 2368. [CrossRef]
8. Chen, J.; Yang, C.; Wang, Q.; Xu, N.; Zhang, T. Nonlinear Ultrasonic Second Harmonic Assessment of Concrete Defects Based on Embedded Piezoelectric Sensors. *Res. Nondestruct. Eval.* **2020**, *31*, 254–270. [CrossRef]
9. Gao, Q.; Jeon, J.Y.; Park, G.; Kong, Y.; Shen, Y. A novel crack localization method for beam structures using piezoelectric sensors. In Proceedings of the 2021 IEEE International Conference on Flexible and Printable Sensors and Systems (FLEPS), Manchester, UK, 20–23 June 2021; pp. 1–4.
10. Ahmadi, J.; Feirahi, M.H.; Farahmand-Tabar, S.; Fard, A.H.K. A novel approach for non-destructive EMI-based corrosion monitoring of concrete-embedded reinforcements using multi-orientation piezoelectric sensors. *Constr. Build. Mater.* **2021**, *273*, 121689. [CrossRef]
11. Perez-Alfaro, I.; Gil-Hernandez, D.; Muñoz-Navascues, O.; Casbas-Gimenez, J.; Sanchez-Catalan, J.C.; Murillo, N. Low-Cost Piezoelectric Sensors for Time Domain Load Monitoring of Metallic Structures During Operational and Maintenance Processes. *Sensors* **2020**, *20*, 1471. [CrossRef] [PubMed]
12. Werner, J.M.; Engelmann, M.; Schmidt, M.; Titsch, C.; Dix, M.; Drossel, W.-G. Comparison of Structural Integrated Piezoceramics, Piezoelectric Patches and Strain Gauges for Condition Monitoring. *Sensors* **2022**, *22*, 8847. [CrossRef]
13. Wallbrink, C.; Hughes, J.M.; Kotousov, A. Application of an advanced piezoelectric strain sensor for crack closure measurement. *Int. J. Fatigue* **2022**, *167*, 107286. [CrossRef]
14. Rogacheva, N.; Sidorov, V.; Zheglova, Y. Piezoelectric Sensor of Small Dynamic Bending Strains. *Buildings* **2024**, *14*, 2447. [CrossRef]
15. Voight, W. *Lehrbuch der Kristallphysik*; Teubner: Berlin, Germany, 1928; 962p.
16. Reuss, A. Berechnung der Fließgrenze von Mischkristallen auf Grund der Plastizitätsbedingung für Einkristalle. *ZAMM-J. Appl. Math. Mech.* **1929**, *9*, 49–58. [CrossRef]
17. Bensoussan, A.; Lions, J.L.; Papanicolaou, G. *Asymptotic Analysis for Periodic Structures*; American Mathematical Society: Providence, RI, USA, 2011; 392p.
18. Sanches-Palencia, E. *Non-Homogeneous Media and Vibration Theory*; Springer: New York, NY, USA, 1980; 393p.
19. Wang, J.; Li, W.; Qin, L.; Zhang, J.; Wei, P. Effects of electrodes and protective layers on the electromechanical characteristics of piezoelectric stack actuators. *Adv. Compos. Lett.* **2019**, *28*, 0963693519877419. [CrossRef]
20. Rogacheva, N.N. Piezoelectric stacks as an effective sensor of small dynamic strains. *IOP Conf. Ser. J. Phys. Conf. Ser.* **2020**, *1425*, 012150. [CrossRef]
21. Available online: <https://www.bostonpiezooptics.com/ceramic-materials-pzt> (accessed on 1 October 2024).
22. Chou, C.C.; Rogacheva, N.N.; Chang, H. Effective electromechanical coupling coefficient for piezoelements. *IEEE Trans. Ultrason. Ferroelectr. Freq. Control.* **1995**, *42*, 630–640.
23. Degefa, T.G.; Wróbel, A.; Płaczek, M. Modelling and Study of the Effect of Geometrical Parameters of Piezoelectric Plate and Stack. *Appl. Sci.* **2021**, *11*, 11872. [CrossRef]
24. Gamboa, B.M.; Guo, R.; Bhalla, A. Piezoelectric stacked transducer evaluation and comparison for optimized energy harvesting. *Ferroelectrics* **2018**, *535*, 8–17. [CrossRef]
25. Wei, T.; Wang, H.; Su, J. Research, design, and analysis of a stacked piezoelectric metamaterial structured sensitive element. *J. Mater. Sci. Mater. Electron.* **2023**, *34*, 1828. [CrossRef]
26. Wang, L.; Jin, J.; Zhang, H.; Wang, F.; Jiang, Z. Theoretical analysis and experimental investigation on a novel self-moving linear piezoelectric stepping actuator. *Mech. Syst. Signal Process.* **2020**, *135*, 106183. [CrossRef]
27. Xu, Q.; Tam, L.M. (Eds.) Chapter 5—Design of a Piezoelectric Energy Harvesting Handrail with Dual Excitation Modes; Mechanical Design of Piezoelectric Energy Harvesters; Academic Press: Cambridge, MA, USA, 2022; pp. 93–113, ISBN 9780128233641. [CrossRef]
28. Harazin, J.; Wróbel, A. Empirical analysis of piezoelectric stacks composed of plates with different parameters and excited with different frequencies. *IOP Conf. Ser. Mater. Sci. Eng.* **2022**, *1239*, 012008. [CrossRef]
29. Liu, X.; Wang, J.; Li, W. Dynamic Analytical Solution of a Piezoelectric Stack Utilized in an Actuator and a Generator. *Appl. Sci.* **2018**, *8*, 1779. [CrossRef]
30. Rodríguez-Fuentes, S.F.; Ferrara-Bello, C.A.; Tecpoyotl-Torres, M. Novel Low-cost Energy Harvester Based on an Arrangement of Piezoelectric. *Actuators Program. Matemática Y Softw.* **2024**, *16*, 22–34. [CrossRef]

**Disclaimer/Publisher’s Note:** The statements, opinions and data contained in all publications are solely those of the individual author(s) and contributor(s) and not of MDPI and/or the editor(s). MDPI and/or the editor(s) disclaim responsibility for any injury to people or property resulting from any ideas, methods, instructions or products referred to in the content.